



UNIVERSITÀ DEGLI STUDI DI MILANO

FACOLTÀ DI SCIENZE E TECNOLOGIE

DIPARTIMENTO DI FISICA

Corso di Laurea triennale in Fisica (L-30)

**Quantum Walks with Time-Dependent Hamiltonians
and their application to the search problem on graph**

Relatore : **Prof. Matteo G.A. Paris**
Correlatore: **Prof. Stefano Olivares**
Correlatrice: **Dott.sa Claudia Benedetti**

Tesi di Laurea di:
Matteo Garbellini
Matricola 885615
Anno Accademico 2019/2020

Abstract

In this thesis we study the properties of quantum walks with time dependent hamiltonian, focusing in particular on the application to the quantum search problem on graph. We compare the time independent and the time dependent approach for two graph topologies, the circular and the complete graph, which represent respectively the worst and best case scenario for the known quantum search. We also investigate the role of the function that regulates the time-dependance of the hamiltonian in the time scaling at which the solution is found. Lastly we exploit the consequences of the adiabatic theorem to study the localization properties of the time-dependent approach.

Contents

Introduction	5
1 Preliminaries	6
1.1. Introduction to graph theory	6
1.1.1 Cycle Graph	8
1.1.2 Complete Graph	8
1.2. Quantum Walks	9
1.3. Grover's Quantum Search	10
1.4. Search by Quantum Walks	13
1.4.1 Search on Complete Graph	15
1.5. Search by Adiabatic Evolution	15
1.5.1 Adiabatic Theorem	16
1.5.2 Global adiabatic evolution	17
1.5.3 Local adiabatic evolution	18
1.6. Impossibility of Adiabatic Quantum Walks	20
2 Quantum Walks with Time-Dependent Hamiltonians	24
2.1. Search with Time-Dependent Hamiltonian	24
2.1.1 Time-Dependent Quantum Walk	25
2.1.2 Interpolating Schedule $s(t)$	26
2.1.3 Multiple Runs for One Search	26
2.2. Selected Topology: Circular and Complete Graph	27

2.3. Characterization of the results: Search, Localization and Robustness	28
2.3.1 Search vs Localization	28
2.3.2 Robustness	29
2.4. Results for the Circular Graph	29
2.4.1 Time-Independent Benchmarks	30
2.4.2 Time-Dependent Results	31
2.4.3 Comparison: Localization	34
2.4.4 Comparison: Search	34
2.4.5 Comparison: Robustness	40
2.5. Results for the Complete Graph	41
2.5.1 Search results from Wong(2016)	41
2.5.2 Localization results	41
Conclusions	42
Appendices	43
Appendix A: Probability Grid Evaluation	43
2.5.3 Optimization Algorithm	43
2.5.4 Schroedinger Solver and Normalization Error	44
Appendix B: Computational Routines	44
Bibliography	46

Introduction

Preliminaries

In this chapter we present the basic theoretical knowledge necessary to understand this thesis. We begin by introducing graph theory, random walks and quantum walks. We then discuss the quantum search problem firstly introduced by Grover and the quantum walks implementation for the unstructured search by Childs and Goldstone. Then we present the adiabatic theorem and its application for computation with adiabatic evolution. Lastly we look at the differences between the quantum walks approach and the adiabatic evolution approach by Ronald and Cerf, which constitutes the basis from which our work is carried on.

1.1. Introduction to graph theory

A graph G is defined as a ordered pair (V, E) , where V is a set of vertices and E is a set of edges, which represent the connection between any two pair of vertices. A vertex is usually indicated by the cursive letter v , and the corresponding edge connecting v to w is given by (v, w) .

A graph can be characterized by many properties. Throughout our work we will only consider *simple graphs* characterized by being *undirected*, namely the edges E are symmetric, having no self loops such that $(v, v) \notin G$ and having no multiple equivalent edges. Additionally we require the graph to be *connected*, where each vertex can be reached by any other, following a path through the available edges. It is then interesting to define the *vertex degree* d_j , that represents, given a vertex j , the number of edges that are incident to the vertex j (in the case of an undirected graph the degree does not depend on the edges incident from or to the selected vertex).

If indeed any two vertices (i, j) are connected by an edge we define them as *adjacent*, and from this we can construct an analytical representation of a graph, given by an N-dimensional square matrix called *adjacency matrix*, usually referred as A . The adjacency matrix is defined as following ¹:

$$A_{ij} = \begin{cases} 1 & \text{if } (i, j) \in G \\ 0 & \text{otherwise} \end{cases} \quad (1.1)$$

which represents the connectivity of the graph.

Furthermore, we can introduce a diagonal matrix D that encodes the informations of the vertex degrees for a particular graph G . Calling the N vertices of the graph as $j = 1, 2..N$ the matrix D is defined as:

$$D = \text{diag}(d_1, \dots, d_N) \quad (1.2)$$

where d_j is the degree of the vertex j . In this particular context a natural operative basis arises, in which one can associate to each ordered vertex of the graph a vector of the standard basis of the N -dimensional vector space.

In order to study the dynamics of the system we introduce a the *Laplacian matrix* L , also known as the *discrete Laplacian operator*. It is defined as

$$L = D - A \quad (1.3)$$

where D is the diagonal degrees matrix and A is the adjacency matrix. The discrete Laplacian operator is the analog of the continuous Laplace operator on discrete domain, and for the finite, undirected, simple and connected graphs that we're going to consider throughout our work, we can characterize it by the following properties:

- L is symmetric given that both D and A are symmetric
- the sum of all elements over a row/column equals to zero

¹If we had to define the adjacency matrix for a general graph the value of A_{ij} is not necessarily equal to one, but a general a_{ij} since it takes into account the possibilities of self loops and multiple equivalent edges. For the simple graphs consider in this thesis the given definition suffices.

- has a null eigenvalue which corresponds to the eigenvector $|\Psi_0\rangle = \frac{1}{\sqrt{N}}(1, 1, \dots, 1)$

In the following paragraphs, we give a brief description of the graphs that will be consider throughtout the work.

1.1.1 Cycle Graph

A N-dimensional cycle graph $Cy(N)$ is a monodimensional structure with periodic boundary conditions $|N+1\rangle = |1\rangle$. The Laplacian is given by

$$L = 2 \sum_{k=1}^N |k\rangle\langle k| - \sum_{k=1}^{N-1} |k\rangle\langle k+1| - \sum_{k=2}^N |k\rangle\langle k-1| - |N\rangle\langle 1| - |1\rangle\langle N| \quad (1.4)$$

A pictorial representation of a cycle graph is given in Fig with the corresponding laplacian matrix.

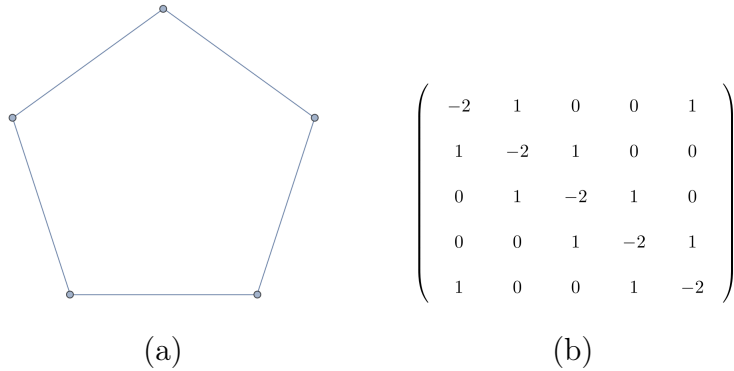


Figure 1.1: Pictorial representation of a cycle graph with 5 nodes (a), and the matricial representation for the Laplacian of $Cy(5)$

1.1.2 Complete Graph

A graph with N vertices is said to be complete if every node is adjacent to all the other N-1 nodes, thus representing a finite bidimensional structure. Its Laplacian matrix is given by:

$$L = (N-1) \sum_{j=1}^N |j\rangle\langle j| - \sum_{k \neq j} |j\rangle\langle k| \quad (1.5)$$

A pictorial representation of a complete graph is given in figure. We will refere to this kind of graph with $C(N)$.

1.2. Quantum Walks

The continuous time quantum walk (CTQW) is the direct analogue of the classical continuous time random walk (CTRW). We begin by considering the classical one, expanding later on the quantum mechanical counterpart.

Let j be a node of a graph G and the initial node, such that the initial state of the system is $|j\rangle$. Then, we denote the transition probability of the walker to go from node j to a node k in a time t with $p_{k,j}(t)$. The state after time t is given by $|j;t\rangle$, such that the overlap with node k is $\langle k|j;t\rangle = p_{j,k}(t)$.

The dynamics resulting in the state $|j;t\rangle$ follows from transition rates per unit time between two nodes. In particular these transition rates are the components of the so-called *transfer matrix* T , namely $T_{ij} = \langle k|T|j\rangle$. If we assume a Markovian process, the following master equation defines the CTRW evolution:

$$\frac{d}{dt}p_{k,j}(t) = \sum_l T_{kl}p_{l,j}(t) \quad (1.6)$$

In the simplest case, where the transition rates for all edges are equal, the transfer matrix is closely related to the Laplacian matrix through :

$$T = -\gamma L \quad (1.7)$$

where γ is the transition rate. The solution of eq. (1.6), along with the normalization constrains $\sum_{k=1}^N p_{k,j}(t) = 1 \forall t$, is given by

$$p_{ij}(t) = \langle k|e^{Tt}|j\rangle = \langle k|e^{-\gamma At}|j\rangle \quad (1.8)$$

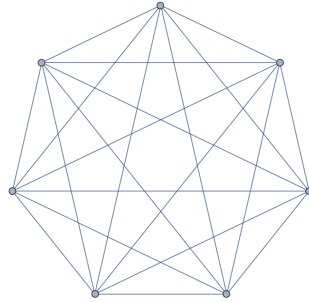


Figure 1.2: Pictorial representation of a complete graph with $N=7$

Turning to quantum mechanics the evolution of any physical system obeys the Schroedinger equation, and QWs represent no exception. The dynamics of the CTQW is governed by a specific Hamiltonian H , such that the Schroedinger equation for the transition *amplitudes* $\alpha_{i,j}(t)$ is given by

$$\frac{d}{dt}\alpha_{i,j}(t) = -i \sum_l H_{k,l} \alpha_{l,j}(t) \quad (1.9)$$

where H is the Hamiltonian of the system, and for simplicity we assume $\hbar = 1$. The formal solution of such differential equation is similarly to the CTRW given by

$$\alpha_{i,j}(t) = \langle k | e^{-iHt} | j \rangle \quad (1.10)$$

where e^{-iHt} is the quantum mechanical time-evolution operator. We immediately notice the similar structure of equations (1.6) and (1.10), with the only difference apart from the imaginary unit that the first is a differential equation for transition probabilities while the latter allows to compute transition amplitudes. The similarity is further pushed by Farhi and Gutmann in 1998 [1], when they proposed to identify the Hamiltonian H of the system with the negative of the classical transfer matrix T , which as we've seen previously is the Laplacian of the graph ²:

$$H = -T = L \quad (1.11)$$

Therefore the Laplacian matrix completely determines the evolution of the quantum system as well as the classical scenario.

1.3. Grover's Quantum Search

In 1997 Lov K. Grover addressed the search problem through a quantum mechanical algorithm [4]. The search problem itself can be formulated in the following way: given an unsorted database containing N items, with only one satisfying a given condition, that one item has to be retrieved. Once an item is examined, it's possible to determine whether it represents the solution or not in just one step. Classically, the most efficient algorithm has to check each and every item in the database individually. If the item checked satisfies the condition the process stops, otherwise it will continue to examine the remaining items until the solution is found. On average, the algorithm will have to check $0.5N$ items before finding

²Please note that in this particular scenario the transition amplitude γ is set to one.

the desired one.

On the other hand, Grover's quantum mechanical approach takes advantage of the *superposition* of states in a quantum system, and by having the input and output in such superposition can find the desired objects in $O(\sqrt{N})$ *quantum mechanical steps*, instead of $O(N)$ classical steps. As we shall see later, this quantum mechanical steps consists of an elementary unitary operation.

Let's look at the algorithm to the quantum search problem more in detail, in particular setting the stage for the search algorithm in terms of an *oracle*, which plays a central role in Grover's search and throughout the entire thesis. Additionally, this allows us to present a very general description of the search procedure, and a geometric way to visualize its action [7].

Suppose we want to search through a search space of N elements, and let's consider the indices of such elements - instead of the actual elements - which clearly are numbers from 0 to $N - 1$. In order to easily store the index in n bits we consider $N = 2^n$, and assume that the particular search problem has only one solution. We can now easily represent one instance of the search, i.e. checking if the item satisfies a particular condition, with a function $f(x)$, where x is the index integer ranging from 0 to $N - 1$. The function is such that if x represents the solution to the search problem $f(x) = 1$, and $f(x) = 0$ if not a solution. In particular we suppose that we are supplied by a quantum *oracle* O with the ability to *recognize* the solution of the search problem. The action of the oracle O is to *mark* the solution by applying a phase, namely $|x\rangle \xrightarrow{O} (-1)^{f(x)}|x\rangle$. In a simplified manner, the quantum search algorithm proposed by Grover consists of repeated application of a quantum subroutine known as the *Grover iteration* or *Grover operator* G defined as:

$$G = (2|\psi\rangle\langle\psi| - I)O \quad (1.12)$$

The questions that arises is what does this Grover operator do. We can show that it can be regarded as a *rotation* in the 2-dimensional space spanned by the beginning vector $|\psi\rangle$ and the vector $|w\rangle$ representing the solution to the search problem. We can then define the normalized state $|\alpha\rangle$ and $|\beta\rangle$:

$$|\alpha\rangle = \frac{1}{\sqrt{N-1}} \sum_{x \neq w} |x\rangle \quad (1.13)$$

$$|\beta\rangle = |w\rangle \quad (1.14)$$

representing respectively, the superposition of all states that are not a solution and the state of the solution. Therefore the initial state $|\psi\rangle$ can be re-expressed by:

$$|\psi\rangle = \sqrt{\frac{N-1}{N}}|\alpha\rangle + \sqrt{\frac{1}{N}}|\beta\rangle \quad (1.15)$$

The effect of G can be understood by realizing that the oracle O performs a *reflection* of $|\psi\rangle$ about the vector $|\alpha\rangle$ in the plane defined by $|\alpha\rangle$ and $|\beta\rangle$. Then, $2|\psi\rangle\langle\psi| - I$ performs another reflection about the vector $|\psi\rangle$. As can be seen in figure?, the product of these two reflections is a rotation. By applying the grover operator k times we can rotate the initial state vector $|\psi\rangle$ close to $|\beta\rangle$, that is, the solution to the search problem. The number of iterations necessary - for which the derivation is not of our interest in the scope of this thesis - is given by $\frac{\pi}{4}\sqrt{N}$.

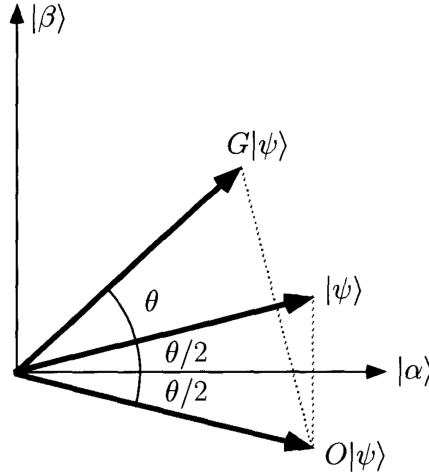


Figure 1.3: Action of the Grover operator G : The figure shows the action of the Grover operator $G = (2|\psi\rangle\langle\psi| - I)O$. Starting from the initial state $|\psi\rangle$ the action of the Oracle O reflects it about the vector $|\alpha\rangle$. Then, the action of $(2|\psi\rangle\langle\psi| - I)$ is an additional reflection about $|\psi\rangle$. The application of the Grover operator for $\pi/4\sqrt{N}$ times rotates the initial state bringing it close to $|\beta\rangle$, that is, the solution of the search problem.

To summarize, G is the rotation in the 2-dimensional space spanned by $|\alpha\rangle$ and $|\beta\rangle$. Repeated application of the Grover operator rotate the initial state vector $|\psi\rangle$ close to $|\beta\rangle$. For applications in the order of $O(\sqrt{N})$, a measurement of the state in the computational basis produces with high probability - very close to 1 - $|\beta\rangle$ as the outcome, that is, the solution to the search problem.

1.4. Search by Quantum Walks

The search problem first introduced by Grover can be reformulated in terms of search based on a continuous-time quantum walk on a graph [2].

In order to do so we need to modify the quantum walk hamiltonian of eq. (1.11) so that the vertex $|w\rangle$ is somewhat special. Therefore, an *oracle hamiltonian* is introduced:

$$H_w = -|w\rangle\langle w| \quad (1.16)$$

that has energy zero for all but the vertex $|w\rangle$ for which it has energy -1 . Therefore the Grover problem becomes finding the ground state of this hamiltonian.

To implement the search we consider the Hamiltonian

$$H = \gamma L + H_w = \gamma L - |w\rangle\langle w| \quad (1.17)$$

where L is the laplacian of the graph G , that as we've seen in section? governs the evolution of the quantum walk.

The quantum search routine works as following:

- we consider the balanced superposition of all possible states, namely

$$|s\rangle = \frac{1}{\sqrt{N}} \sum_j |j\rangle \quad (1.18)$$

- we run the quantum walk for a time t_f and find the corresponding evolved state using the hamiltonian H

$$|\psi(t_f)\rangle = U(t_f)|s\rangle = \exp\left\{-\frac{i}{\hbar} H t_f\right\} |s\rangle \quad (1.19)$$

(Note that this evolution is valid only for time-independent hamiltonians.)

- we then measure the state onto the target $|w\rangle$ and find the corresponding probability

$$p = |\langle w|\psi(t_f)\rangle|^2 \quad (1.20)$$

The objective is to find the optimal value of γ so that the success probability $|\langle w|\psi(t_f)\rangle|^2$ is as close as possible to 1 for the smallest t_f .

We can turn our attention on trying to understand why we should expect this

algorithm to give a success probability for some values of γ, t_f . To motivate this we need to frame the problem in terms of Hamiltonian spectrum. In particular we look at the two extremes, namely $\gamma \rightarrow \infty$ and $\gamma \rightarrow 0$.

- as $\gamma \rightarrow \infty$ the contribution of H_w is somewhat negligible, to the point that the ground state of H is $|s\rangle$ ³
- on the other hand, if $\gamma \rightarrow 0$ the contribution of the Laplacian to the overall Hamiltonian H disappears and thus the ground state of H is close to $|w\rangle$

We expect that for some intermediate γ the ground state will transition from $|w\rangle$ to $|s\rangle$ and thus could have substantial overlap on both for a certain value of γ . Additionally, if the first excited states have substantial overlap at such values of γ , then the Hamiltonian will drive transitions between two states, thus rotating the state from $|s\rangle$ to one with substantial overlap with $|w\rangle$, giving the success probability that we previously talked about. In particular this transition will happen in a time that depends on the Hamiltonian eigenvalues separation between the first and ground state, namely $1/(E_1 - E_0)$.

This is a good description of the algorithm if the dimension of the graph is sufficiently high. However, if we consider a d -dimensional lattice with d independent of N we still see that for a critical value of γ the state switches from the ground state to the first excited state, but for $d < 4$ the $|w\rangle$ state does not have substantial overlap on the ground and first excited state, thus the algorithm does not work.

Comments on the oracle H_w : The oracle introduced in this fashion is exactly the continuous-time version of the reflection R_w in Grover's algorithm [10] because by itself it only evolves the marked vertex $|w\rangle$ by a phase

$$e^{-i|w\rangle\langle w|t}|w\rangle = e^{-it}|w\rangle \quad (1.21)$$

while leaving the other vertices unchanged, thus making this the continuous-time version of a yes/no oracle.

³Note that regardless of the graph topology considered, $|s\rangle$ is the ground state of the Laplacian, with $L|s\rangle = 0$.

1.4.1 Search on Complete Graph

We now look at the complete graph which can be thought of having dimension proportional to N and represents the simplest example of the quantum walk search application [2].

We begin by noticing that adding a multiple of the identity matrix to the Laplacian only contributes a global unobservable phase. We add $-NI$ so that:

$$L - NI = N|s\rangle\langle s| \quad (1.22)$$

This gives us the following Hamiltonian:

$$H = -\gamma N|s\rangle\langle s| - |w\rangle\langle w| \quad (1.23)$$

In particular we know that this hamiltonian acts non-trivially in a two dimensional subspace spanned by $|s\rangle$ and $|w\rangle$, thus making it stright-forward to compute its spectrum. If we use the $\{|w\rangle, |r\rangle\}$ basis, the hamiltonian can be expressed in the following way:

$$H = \frac{-1}{N} \begin{pmatrix} N+1 & \sqrt{N-1} \\ \sqrt{N-1} & N-1 \end{pmatrix} \quad (1.24)$$

Applying the time-evolution operator to the initial state $|s\rangle$, the system at time t will be

$$|\psi(t)\rangle = e^{it} \begin{pmatrix} \frac{1}{\sqrt{N}} \cos(\frac{t}{\sqrt{N}}) + i \sin(\frac{t}{\sqrt{N}}) \\ \sqrt{\frac{N-1}{N}} \cos(\frac{t}{\sqrt{N}}) \end{pmatrix} \quad (1.25)$$

and for $t = \pi\sqrt{N}/2$ the system reaches a success probability of 1, namely

$$p = \left| \langle w | \psi(t) \rangle \right|_{t=\pi\sqrt{N}/2}^2 = \left| \langle w | i e^{it} w \rangle \right|^2 = 1 \quad (1.26)$$

recalling that in the 2-dimensional subspace $w = (0, 1)$. Thus the walk rotates the state from $|s\rangle$ to $|w\rangle$ in $O(\sqrt{N})$.

1.5. Search by Adiabatic Evolution

We now address the computation by adiabatic evolution firstly introduced by Farhi et al., that takes advantage of the adiabatic theorem to find the solution of a computational problem [3]. We begin by looking at the *adiabatic theorem* and its implication. Then, an overview of the adiabatic implementation of the

algorithm for solving the unstructured search problem is given which has a time scaling of $O(N)$. Lastly, we see how applying the adiabatic theorem *locally* can lead to a time of order $O(\sqrt{N})$ which is optimal.

1.5.1 Adiabatic Theorem

A quantum system evolves according to the Schroedinger equation

$$i \frac{d}{dt} |\psi(t)\rangle = H(t) |\psi(t)\rangle \quad (1.27)$$

and defining the instantaneous eigenstates and eigenvalues of $H(t)$ by

$$H(t) |l; t\rangle = E_l(t) |l; t\rangle \quad (1.28)$$

such that $E_0(t) \leq E_1(t) \leq \dots \leq E_{N-1}(t)$.

The adiabatic theorem states that if the gap between the two lowest energy levels, $E_1(t) - E_0(t) > 0$, is strictly greater than zero then for $T \rightarrow \infty$ the probability of being in the ground state is equal to one, namely

$$\lim_{T \rightarrow \infty} |\langle l=0; t=T | \psi(T) \rangle| = 1 \quad (1.29)$$

This means that if the system is chosen to evolve at a slow enough rate, the instantaneous hamiltonian will remain in the ground state through the evolution. It is useful to consider a smooth one-parameter hamiltonian $H(s)$ such that $s = t/T$, with $t \in [0, T]$ so that $s \in [0, 1]$. Let's now define the energy minimum gap by

$$g_{min} = \min_{0 \leq s \leq 1} (E_1(s) - E_0(s)) \quad (1.30)$$

In addition we can find a time lower bound T^* such that for $T \gg T^*$ the probability is arbitrarily close to 1, in detail

$$T \gg \frac{\varepsilon}{g_{min}^2} \quad (1.31)$$

where

$$\varepsilon = \max_{0 \leq s \leq 1} \left| \left\langle l=1; s \left| \frac{dH(s)}{ds} \right| l=0; s \right\rangle \right| \quad (1.32)$$

Let's now discuss how to take advantage of the adiabatic theorem introducing the usual way in which the adiabatic evolution is implemented. It is often presented a problem hamiltonian H_P whose ground state is not so straight forward to find;

on the other hand we can prepare the system in a beginning hamiltonian H_B whose ground state is known. The problem hamiltonian encodes the solution of the problem, while the beginning hamiltonian is a tool for easily preparing the state to be evolved. The adiabatic implementation then consists, assuming that the ground state of H_P is unique, in having a time dependent hamiltonian $H(s)$ such that

$$H(s) = (1 - s)H_B + sH_P \quad (1.33)$$

In this way we can prepare for $s = 0$ the system in H_B and let it evolve so that for $s = 1$ it reaches H_P . Thanks to the adiabatic theorem, if it's made to evolve sufficiently slowly we will find ourself in the ground state of the problem hamiltonian, which is exactly the solution.

1.5.2 Global adiabatic evolution

Let's now apply what just seen to the unsorted search problem [8]. As done in Section? we consider an unsorted database of N elements such that $N = 2^n$, so that the elements in this particular basis can be written as $|i\rangle$, with $i = 0, \dots, N-1$. The marked state can be then denoted as $|w\rangle$, and we begin by considering the initial state as the superposition of all the elements $|i\rangle$:

$$|\psi_0\rangle = \frac{1}{\sqrt{N}} \sum_{i=0}^{N-1} |i\rangle \quad (1.34)$$

With this in mind we design two particular Hamiltonians H_0 and H_w such that $|\psi_0\rangle$ is the ground state of the first while $|w\rangle$ is the ground state of the latter:

$$H_0 = I - |\psi_0\rangle\langle\psi_0| \quad (1.35)$$

$$H_w = I - |w\rangle\langle w| \quad (1.36)$$

The time-dependent Hamiltonian follows from the adiabatic implementation discussed in Section?, where H_0 is the beginning hamiltonian while H_w is the problem hamiltonian. It thus consists in a linear interpolation between H_0 and H_w :

$$H(t) = (1 - s)H_0 + sH_w \quad (1.37)$$

where $s = t/T$ is the linear interpolating schedule.

The search routine runs as usual, beginning with preparing the system in the

state $|\psi(0)\rangle = |\psi_0\rangle$ and then applying the Hamiltonian $H(t)$ for a time T . We're interested in finding the time-dependent condition such that the system evolves sufficiently slowly, allowing us to find the solution $|w\rangle$ with high probability. First, we determine the quantity $\langle \frac{dH}{dt} \rangle$:

$$\left\langle \frac{dH}{dt} \right\rangle_{0,1} = \frac{ds}{dt} \left\langle \frac{dH}{ds} \right\rangle_{0,1} = \frac{1}{T} \left\langle \frac{dH}{ds} \right\rangle_{0,1} \quad (1.38)$$

We then find the eigenvalues of the Hamiltonian and determine the separation g between the ground state and first excited one, namely E_1 and E_0 , as a function of the interpolating schedule s :

$$g = \sqrt{1 - 4 \frac{N-1}{N} s(1-s)} \quad (1.39)$$

We're interested in the minimum gap g_{\min} which is found for $s = 1/2$. Additionally we find that $\left| \left\langle \frac{dH}{ds} \right\rangle_{0,1} \right| \leq 1$, therefore Eq? becomes:

$$\frac{\left| \left\langle \frac{dH}{ds} \right\rangle_{0,1} \right|}{g_{\min}^2} \leq \varepsilon \quad (1.40)$$

so that the adiabatic condition is verified, and thus the hamiltonian stays in the ground state at all times, provided that $T \geq N/\varepsilon$. Therefore the computation time is of order N , showing no speed up compared to the classical search.

1.5.3 Local adiabatic evolution

Roland and Cerf showed that the adiabatic evolution can be improved by applying the adiabatic condition of eq. (1.40) locally instead of globally [8]. If we look at the plot of the separation g we see that the adiabatic condition is critical only for $s = 1/2$ where it reaches its minimum. At the beginning and at the end of the evolution the separation is large enough so that the adiabatic condition and thus the time necessary for the system to evolve adiabatically is small, allowing for better time scaling. The improvement comes in the form of the interpolating schedule, following the idea that it should be steeper for large separation g and flatter (more than linear) for small separation around $s = 1/2$. Let's see how can this be done.

We divide the interval $[0, t_f]$ into infinitesimal intervals dt and adapt the evolution

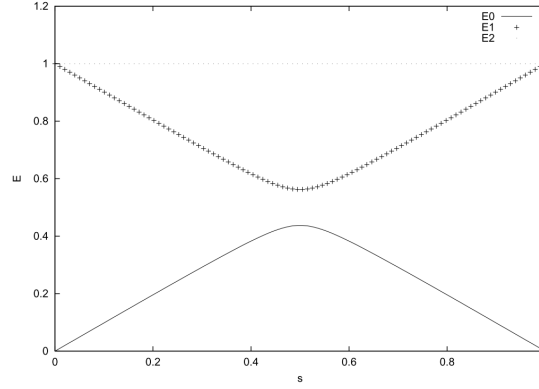


Figure 1.4: Eigenvalue separation of the time-dependent Hamiltonian $H(s)$ as a function of the reduced time s , for $N=64$. *Figure from Roland and Cerf [8]*

rate $\frac{ds}{dt}$ to the local adiabatic condition. In this way we can find the optimal $s(t)$, with boundary conditions $s(0) = 0$ and $s(t_f) = 1$. We find the new adiabatic condition for all time t :

$$\left| \frac{ds}{dt} \right| \leq \varepsilon \frac{g^2(t)}{\left| \left\langle \frac{dH}{ds} \right\rangle_{0,1} \right|} \quad (1.41)$$

Using eq. (1.39) and $\left| \left\langle \frac{dH}{ds} \right\rangle_{0,1} \right| \leq 1$ and Hamiltonian is chosen to evolve with the interpolating schedule that is solution of the following differential equation (with $\varepsilon \ll 1$):

$$\frac{ds}{dt} = \varepsilon g^2(t) = \varepsilon \left[1 - 4 \frac{N-1}{N} s(1-s) \right] \quad (1.42)$$

After integration we get the following

$$t = \frac{1}{2\varepsilon} \frac{N}{\sqrt{N-1}} \left[\arctan(\sqrt{N-1}(2s-1)) + \arctan \sqrt{N-1} \right] \quad (1.43)$$

By inverting we find the interpolating schedule $s(t)$ as can be seen in fig. 1.5. In order to determine the computation time of this algorithm. To do so we evaluate $s = 1$ and in the approximation that $N \gg 1$ we get:

$$T = \frac{\pi}{2\varepsilon} \sqrt{N} \quad (1.44)$$

which represents a great improvement on Eq?. Indeed we have a quadratic speed up compared to the global adiabatic evolution, and thus this algorithm can be seen as the adiabatic implementation of the Grover's search algorithm.

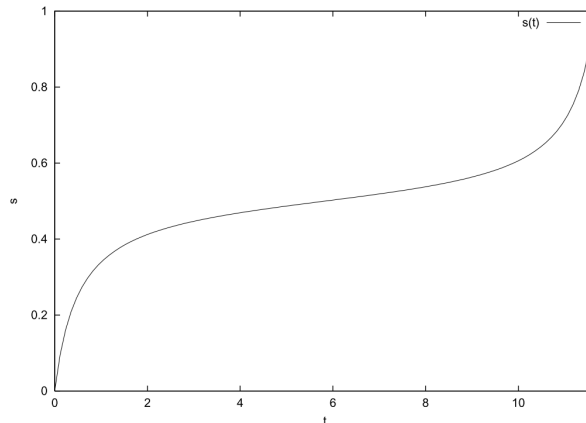


Figure 1.5: Eigenvalue separation of the time-dependent Hamiltonian $H(s)$ as a function of the reduced time s , for $N=64$. *Figure from Roland and Cerf [8]*

1.6. Impossibility of Adiabatic Quantum Walks

In this section we show that an *adiabatic quantum walks* based search algorithm cannot be implemented with the usual Grover's oracle and requires a more sophisticated structure. This section, based on a paper by Wong et al. [10], sets the basis on which our work takes place.

In the previous sections we discussed Grover's original discrete-time search algorithm (GR), Farhi and Gutmann's quantum walk analogue (FG) and Roland and Cerf's adiabatic analogue (RC). Throught the discussion we analyzied the systems in a 2-dimensional subspace spanned by $\{|w\rangle, |r\rangle\}$. This allows to visualize the evolution of the quantum algorithm on the two dimensional Bloch sphere and compare the path taken by each different approach. In particular we notice that the original Grover's algorithm and the Roland and Cerf's local adiabatic evolution follow the same path on the xz -plane since they both always have real coefficients, as can be seen in Figures 1.6a and 1.6b respectively. On the other hand the quantum walk formulation of Farhi and Gutmann has an unmeasurable complex phase thus it evolves on a different path on the yz -plane, see Figure 1.6c.

This substantial difference of the path taken by the different algorithms is exactly what Wong et al. investigate, in particular with the goal of determine which adiabatic algorithm does follow the same path of the quantum walk algorithm of Farhi and Gutmann in order to implement an adiabatic quantum walk based

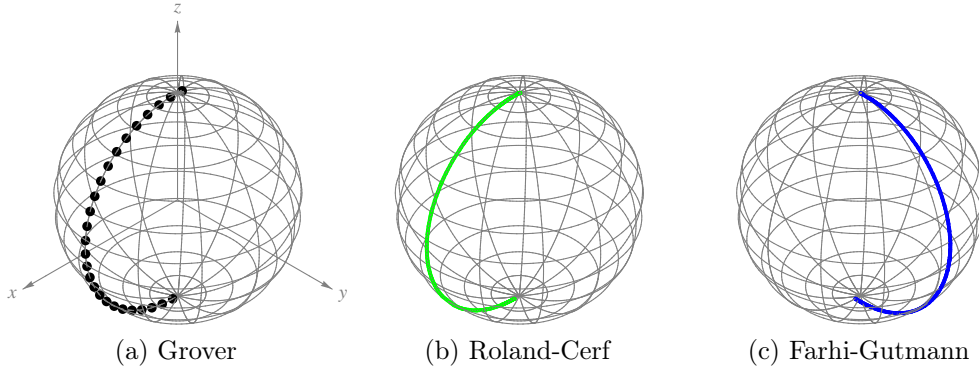


Figure 1.6: **Evolution of the quantum algorithms on the Bloch sphere.** The figure shows the evolution of quantum algorithm on the Bloch sphere with marked vertex $|w\rangle$ at the North Pole and the equal superposition of the unmarked vertices $|r\rangle$ at the South Pole, and $N = 1024$: (a) Grover's original discrete-time search algorithm, (b) Roland and Cerf's local adiabatic evolution analogue and (c) Farhi and Gutmann's quantum walk analogue. *Wong et al. (2016) [10]*

search algorithm.

To do so they constructed an hamiltonian starting from the following states, with the first represents the ground state and the latter the first (and only) excited state - remember that the Grover's search rotates the initial state over the final state, thus the first excited state is the orthogonal of the ground state.

$$|\psi_0(t)\rangle = \alpha(t)|w\rangle + \beta(t)|r\rangle \quad (1.45)$$

$$|\psi_1(t)\rangle = \beta(t)|w\rangle - \alpha^*(t)|r\rangle \quad (1.46)$$

where the coefficients are given by the components of $|\psi_0(t)\rangle$ of eq. (1.25)⁴. The hamiltonian is then given by the linear combination of $|\psi_0(t)\rangle$ and $|\psi_1(t)\rangle$:

$$H(t) = \lambda_0|\psi_0\rangle\langle\psi_0| + \lambda_1|\psi_1\rangle\langle\psi_1| \quad (1.47)$$

which allows to determine the final time-dependent *adiabatic* hamiltonian - where the time-dependence is given by the interpolating schedule $s(t)$:

$$H(s) = \sqrt[4]{\frac{s(1-s)}{4\varepsilon^2 N}} \left[(1-s)H_0 + sH_f + \sqrt{s(1-s)}H_e \right] \quad (1.48)$$

where the interpolating schedule is given by $s(t) = \sin^2\left(\frac{t}{\sqrt{N}}\right)$. Indeed the system

⁴Note that the global phase e^{it} is dropped.

evolves from $t = 0$ to $t = \frac{\pi}{2}\sqrt{N}$ as we would expect. Looking closely the Hamiltonian H_0 is the beginning hamiltonian, H_f is the final hamiltonian - encoding the solution of the search problem - and H_e is an *extra* hamiltonian, a common tecnique for manipulating the evolution of the path of adiabatic algorithms⁵. Let's now look at the consequences of this Hamiltonian, looking at H_0 , H_f and H_e individually.

H_0 has ground state $|s\rangle$ and excited state $|s^\perp\rangle$ with respective eigenvalues -1 and $+1$, thus the hamiltonian can be written as:

$$H_0 = |s^\perp\rangle\langle s^\perp| - |s\rangle\langle s| \quad (1.49)$$

Similarly, the final Hamiltonian H_f has ground state $|w\rangle$ and excited state $|r\rangle$ with eigenvalues $+1$ and -1 :

$$H_f = |r\rangle\langle r| - |w\rangle\langle w| \quad (1.50)$$

It's immediate to notice that these two hamiltonian look fairly similar to the initial and final hamiltonian of the standard adiabatic quantum search algorithm of Equations (1.35) and (1.36). Although the similarities look at first sight promising, the extra Hamiltonian H_e and the interpolating schedule $s(t)$ change completely the evolution of the system. In particular, if we look at the Hamiltonian H_e - given by:

$$H_e = 2i\sqrt{\frac{N-1}{N}}(|r\rangle\langle w| - |w\rangle\langle r|) \quad (1.51)$$

we see that rather than having the standard yes/no oracle given by $|w\rangle\langle w|$, this extra hamiltonian introduces a more powerful structure, driving the evolution between $|w\rangle$ and $|r\rangle$ insted of just applying a phase to the targer state $|w\rangle$ like in the standard Grover's algorithm. This is a confirmation that the oracle is no more the usual Grover's yes/no oracle, and althought this a proof that an adiabatic evolution following the quantum walk path does exists it abandons the usual notion of the oracle and does not solve the search problem itself as originally posed by Grover.

The difference between the Quantum Walks and the Adiabatic Evolution approach is not a measure of the performance of the algorithms, since both, individually,

⁵The extra hamiltonian commonly appears as $s(s-1)$, while the one considered in this scenario is given by the square root of such value [10].

solve the Grover's problem in $O(\sqrt{N})$ time, but illustrate that the “*how* they compute is different, even though *what* they compute is the same ” [10].

Although the work by Wong et al. showed that is not possible to implement an adiabatic quantum walk algorithm that solves the search problem, it leaves space to a time-dependent algorithm *inspired* by the adiabatic evolution but that it's free from the constraints of the adiabatic condition. From this last consideration we develop the next chapter that summarized the work done and gives some interesting insights and properties of the quantum walks search algorithm with time-dependent hamiltonians.

Quantum Walks with Time-Dependent Hamiltonians

The main purpose of this thesis is to study quantum walks with time dependent hamiltonians, focusing in particular on their application to the spatial search problem on graph. The general idea is trying to improve a time-independent implementation of quantum walks search using a time-dependent hamiltonian analogous to the one used in the adiabatic evolution. In order to determine whether this new approach produces successfull results we study two selected graph topology: the circular graph, for which the time-independent approach is not able to solve the search problem, and the complete graph for which the search problem is solved for both the time-independent and adiabatic evolution approaches.

We compare the two methods for the optimized-search, localization - which represents a search without needs to optimize the time - and a measure of robustness.

2.1. Search with Time-Dependent Hamiltonian

In Section? we discussed the use of quantum walks for the spatial search problem [2] and the application to the complete graph where the search problem is solved. We then illustrated how the adiabatic theorem can be used to solve computational problems with an adiabatic evolution of a quantum system [3]. Efforts to combine the two approaches showed that the search problem can be solved only with structures stronger than the usual Grover's oracle [10], thus making an *Adiabatic-Quantum-Walk-Search* impossible. However this leaves space

to a merely time-dependent quantum walk search, that takes advantage of a time-dependent implementation similar to the adiabatic evolution but that is not bounded to the strict adiabatic-theorem conditions and the limitation of the standard Grover's oracle.

2.1.1 Time-Dependent Quantum Walk

Following from the adiabatic evolution discussed in the preliminaries, we consider a search hamiltonian that interpolates between an initial hamiltonian, i.e. the laplacian of the graph L , and the final oracle hamiltonian $H_w = \gamma|w\rangle\langle w|$

$$H(s) = (1 - s)L - s\gamma|w\rangle\langle w| \quad (2.1)$$

where the interpolation schedule $s = s(t)$ goes from 0 to 1 as the time t goes from 0 to the runtime t_f .

In order to find the evolved ground state of the beginning hamiltonian we need to determine the evolution operator that for a time-dependent hamiltonian is given by:

$$S(t, t_0) = \text{Texp} \frac{1}{i\hbar} \left\{ \int_{t_0}^t dt' H(t') \right\} \quad (2.2)$$

where T is the time-ordering. Since we're only interested in the evolved state, having the exact evolution operator is somewhat irrelevant. Additionally for the circular graph - which represents the main topology studied in this thesis - the search hamiltonian does not show any particular properties making an analitical derivation of the operator not possible. We therefore proceed by solving the differential Schroedinger equation:

$$i \frac{d}{dt} |\psi(t)\rangle = H |\psi(t)\rangle \quad (2.3)$$

Recalling that we're dealing with matrices and vectors in an N-dimensional Hilbert space, we solve N-differential equations of the form

$$\frac{d}{dt} |\psi_i(t)\rangle = \sum_j H_{ij} |\psi_j(t)\rangle \quad (2.4)$$

with the boundary conditions $|\psi_i(0)\rangle = |\psi_i\rangle$.

From a numerical point of view this approach is also much simpler than other

direct methods of evaluating the evolution operator, such as the Dyson Series or Magnus Expansion.

2.1.2 Interpolating Schedule $s(t)$

As pointed by Wong the interpolating schedule $s(t)$ plays a crucial role in the evolution of the system and in the overall scaling of the algorithm. The original adiabatic evolution by Farhi and Gutmann. [3] uses a linear interpolating schedule defined as $s(t) = \frac{t}{t_f}$. Ronald and Cerf show that in order to obtain a quadratic speedup for the complete graph a non linear schedule is essential [8][5].

Thus, from a linear interpolating schedule we begin considering, somewhat naively, quadratic and cubic schedules:

$$s(t) = \sqrt{\frac{t}{t_f}} \quad s(t) = \sqrt[3]{\frac{t}{t_f}} \quad (2.5)$$

We then consider the interpolating schedule analitically derived by Ronald and Cerf for the unstructured search (complete graph) given by :

$$t = \frac{1}{2\epsilon} \frac{N}{\sqrt{N-1}} \left[\arctan(\sqrt{N-1}(2s-1)) + \arctan\sqrt{N-1} \right] \quad (2.6)$$

By inverting the function, $s(t)$ is obtained as plotted in fig. 2.1(a)

The shape of this interpolating schedule comes from the gap $g(s)$ between the lowest two eigenvalues, changing faster when the gap is large, while it evolves slower when the gap is small. We therefore take these key aspects of $s(t)$ - derived for the unstructured search - and consider a similar interpolating schedule defined as follow

$$s(t) = \frac{1}{2}(2(x-1)^3 + 1) \quad (2.7)$$

2.1.3 Multiple Runs for One Search

To give a complete picture of the usefulness of the time-depended approach, we consider the possibility of repeating the search multiple times. If the probability at which the solution is found is $p = 1$ the search is perfect and the problem is solved. However, if the proabability is less than one, i.e. imperfect search, the problem can be solved by searching multiple times . Since the results of the

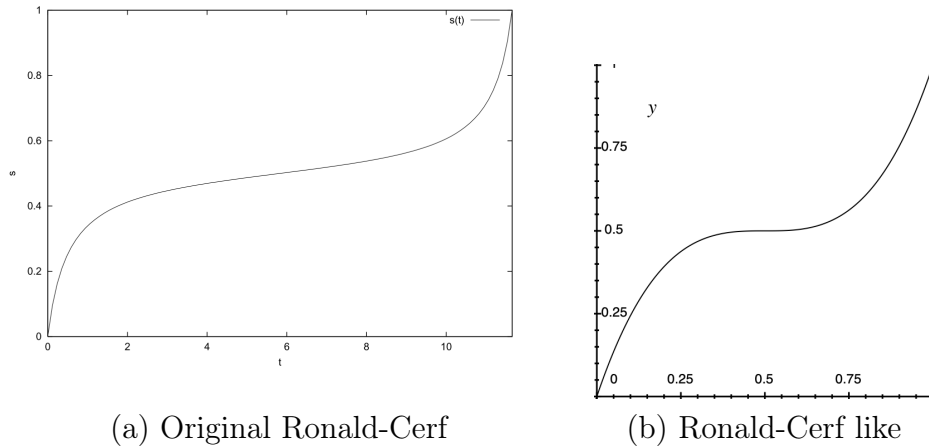


Figure 2.1: **Ronald and Cerf’s interpolating schedule (a) and our Ronald-Cerf like schedule (b).** These figures show the difference between the original interpolating schedule derived by Ronald and Cerf for the unstructured search (left) and our Ronald-Cerf like schedule(right). Although quite different we study the effects of this particular non-linear interpolating schedule and compare it with the linear one used by Farhi and Gutmann [3].

search are checked independently, a single successful search is sufficient, and this kind of routine is efficient as long as the probability $|\langle\psi(t_f)|w\rangle|^2$ is greater than $1/\text{poly}(N)$ (where N is the dimension of the graph) [5].

Repeating the search multiple times does however come at a cost. It is indeed necessary to take into account for a non-zero *initialization* time t_{init} to prepare the system in the correct state as well a physical time for the measurement. Therefore, computing multiple searches with small t_f becomes less efficient than less searches with larger t_f , where the quantity t_{init} makes a lesser contribution to the overall t_f . Clearly this consideration is particularly relevant for increasing graph size.

2.2. Selected Topology: Circular and Complete Graph

Throughout our analysis we will focus the attention on two selected graph topology, the ring graph (R) and the complete graph (C).

As previously discussed in Section? the **complete graph** represents the best case scenario since it has been shown to solve the search problem both for the

standard time-independent quantum walk approach [2] and the local adiabatic evolution [8], with a quadratic speed up. An adiabatic implementation of the quantum walk search does not work with the usual Grover's oracle requiring a more elaborate structure [10], however as we shall later see a merely time-dependent approach might give promising results in terms of robustness.

The **circular graph** on the other hand is not able to solve the search problem with the time-independent approach, and can give some interesting insights with the application of the time-dependent quantum walk search.

The choice of graph topology is therefore based on the idea of giving results at either side of the spectrum of 2-dimensional graphs, trying to improve a non-working approach on one side, and get some interesting insights on an already perfect-search approach on the other.

2.3. Characterization of the results: Search, Localization and Robustness

Firstly it's necessary to define what type of results we're looking for. We begin by showing the difference between **search** and **localization**. Then we introduce a (not-so-rigorous) measure for the **robustness** of the search algorithm.

2.3.1 Search vs Localization

Before looking at the results it's necessary to characterize two particular classes of results, the **search** and the **localization**, that help us decide whether the time-dependent approach does bring any advantages.

- the (optimized) **search** describes the usual search, namely the finding of the solution with high probability (possibly unitary) for the smallest time as possible. As previously mentioned we also take into account the possibility of repeating the search multiple times.
- the **localization** describes the finding of the solution with high probability without the need to optimize the time. This description becomes necessary if we take into account the adiabatic nature of the time-dependent approach, that guarantees unitary probability for large enough t_f .

2.3.2 Robustness

We've seen that the probability of a search problem depends on the time t_f at which the quantum state is measured and the parameter γ . The optimal probability, i.e. highest possible, clearly is given by the optimal combination $t_f - \gamma$, and since the time t_f should not be bound to errors give it's the time at which the state is measured, fluctuations in the probability are necessarily caused by fluctuations in the γ parameter.

Following from [9] we define the **robustness** as quantitative measure representing the variation on the probability due to some perturbation/noise on γ . We begin by finding the optimal probability P , evaluated with the single or multiple run for one search approach. For the corresponding (t_f, γ) combination we evaluate the robustness as follows:

$$R^\pm = P(t_f, \gamma) - P(t_f, \gamma \pm \delta) \quad (2.8)$$

where δ is some positive perturbation of the γ parameter. As we shall later see this quantity is given in terms of some percentage of γ . To find a unique value for the robustness an average of R^\pm is done:

$$R = \frac{R^+ + R^-}{2} \quad (2.9)$$

The quantity R should be positive, since the (t_f, γ) combination should produce the highest probability possible. We also that the perturbation on the parameter has equal probability of being positive or negative, thus the average ponderates between these two possibilities.

It is necessary however to remember that the value R does not have any absolute physical significance, but fits well for our specific scenario where the interest is focused on the comparison between two specific approaches. Therefore this quantity will be solely used to characterize a particular approach as **more** or **less robust**.

2.4. Results for the Circular Graph

We now address the results for the circular graph. We begin by computing benchmarks for the time-independent hamiltonian approach; this should give us

a good starting point for the comparison. Then we consider the time-dependent hamiltonian and evaluate the necessary data. We compare the two approaches, beginning from the Localization, followed by the Search which requires the introduction of a new quantity that takes into account the possibility of doing multiple runs for one search. Lastly we study the robustness of the time-dependent approach and determine whether the newly introduced hamiltonian makes the search more robust than the time-independent search.

2.4.1 Time-Independent Benchmarks

The first step of the analysis is to compute time-independent benchmarks. We computed the probability over a time-beta grid, with $T \in [0, N]$ and $\gamma \in [0, 2.5]$, where N is the dimension of the graph considered. An initial run of the probability distribution showed that the probability does not increase with time, thus the need to evaluate for t_f greater than $T = N$ proved to be unnecessary. In addition Grover algorithm for the unstructured search (and the complete graph) scales \sqrt{N} and the Farhi and Gutmann's adiabatic evolution scales like N , thus focusing on $T \leq N$ made much more sense. **Figure of probability distribution for sampled γ**

Throughout the analysis we will consider graphs up to $N = 71$, with only odd dimensions which makes a easier oracle placement. Additional considerations and reasoning for the time-gamma grid can be found in Appendix A.

To display the results in an intuitive way we used a heatmap plot, which gives a good idea on the probability distribution for varying combinations of (T, γ) :

Comments on the probability distribution

From the heatmap plot we see that the probability distribution does not increase smoothly with increasing time, but shows peaks (dark regions) and valleys (lighter regions). Additionally dark regions are scattered throughout the grid and not necessarily for large t_f . We will later see that this is somewhat a weakness of the time-independent approach, since a small variation of the parameter β , which represents as previously mentioned the deepness of the well or an energy parameter, leads to possibly great variation of the probability.

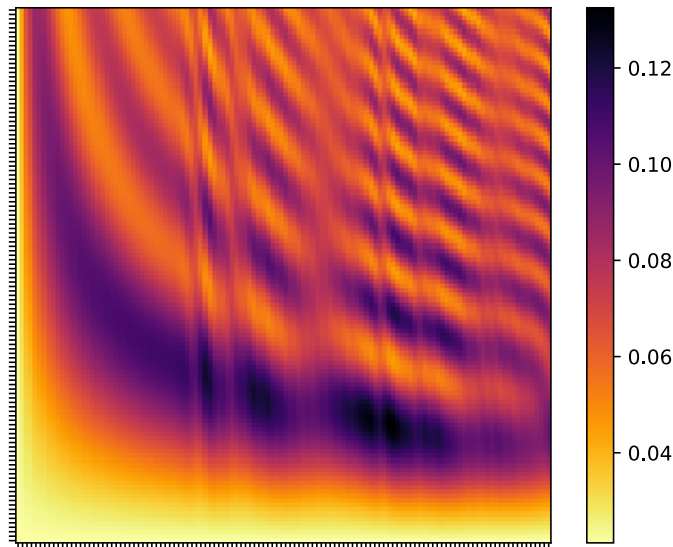


Figure 2.2: **Probability heatmap plot for the time-independent hamiltonian.** The figure shows the probability distribution for a circular graph of $N=47$ evaluated using the time-independent hamiltonian, providing thus the necessary benchmark. Note that dark color do not represent probabilities close to one, but only higher probability regions.

2.4.2 Time-Dependent Results

Similarly we computed the grid probability using the time-dependent hamiltonian previously introduced. To easily comparing the two methods we opted to consider the same time $T = N$, and from an initial run we discovered that the γ parameter affected similarly the probability (**A plot is needed to support this statement**), namely the probability tended to be higher for smaller values of γ , thus we used approximately the same range.

The grid-probability is evaluated for all the interpolating schedules $s(t)$ previously discussed, and an intuitive heatmap plot is outputted.

Comments on the probability distribution

Compared to the time-independent hamiltonian approach we can clearly see that the probability distribution is smoother (has no valley and peaks) both for constant γ (any horizontal section) and constant t_f (any vertical section). If we look at the different interpolating schedules it's immediately evident that the cbt and sqrt schedules perform poorly compared to the linear one. On the other

hand the Ronald-Cerf schedule performs in a similar way in terms of the highest probability found, but has a significantly different probability distributio, that might affect its robustness.

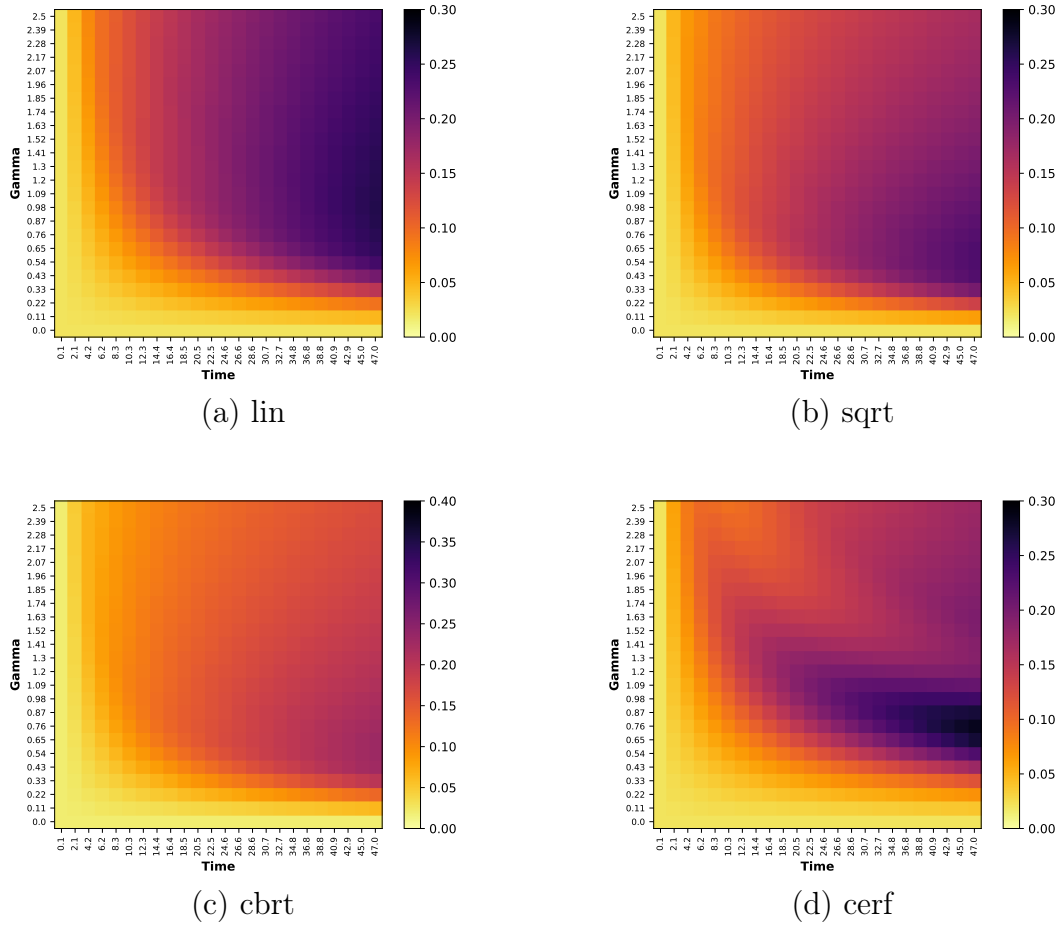


Figure 2.3: **Probability heatmap plot for the time-dependent hamiltonian, for different shapes of $s(t)$.** The figure shows the probability distribution for a circular graph of $N=47$ evaluated using the time-dependent hamiltonian using the following step functions (a) linear, (b) $\sqrt{t/T}$, (c) $\sqrt[3]{t/T}$ and (d) Ronald-Cerf(3). Note that the color gradient is normalized to $p=0.3$ to accentuate the difference in probability between different regions.

2.4.3 Comparison: Localization

We now compare the localization properties of the two algorithm. As we mentioned in the comments to the probability distributions of the time-independent and time-dependent approaches we discovered the following:

- **Time-Independent QW:** the time-independent based search is not able to solve the search problem with a single iterations, thus making it necessary to run multiple searches. This implies that the approach does not show any localization properties, in fact the probability does not increase with time as in the time-dependent approach.
- **Time-Dependent QW:** the time-dependent based search on the other hand because of the adiabatic theorem does solve the search problem with a single iterations, although that happens for fairly large t_f .

Although the time-dependent approach is able to get to unitary probability in a fairly large t_f , it is able to produce large enough probabilities in much less time, as we can see from this plot. This is a consequence of the fact that the probability does not grow linearly with time, thus needing larger t_f closer it gets to $P = 1$. **A plot is needed**

2.4.4 Comparison: Search

In order to compare the two approaches for the search it is clear that we cannot simply consider the time at which the solution is found with unitary probability, since that particular t_f is not optimized for the time-dependent approach and does not exist for the time-independent one. Therefore, as previously mentioned we consider the possibility of doing multiple runs for one search. For this reason we introduce the following quantity

$$\min \left(\frac{t_f}{p} \right) \quad (2.10)$$

where $1/p$ is the number of iterations necessary to get to unitary probability (statistically), and combining it with t_f gives the total time necessary. Optimizing over the combination of t_f and p gives the smallest time necessary to get to unitary probability using the multiple search approach. Additionally, the number of iterations $\text{iters} = 1/P$ might give some useful insights on the performance of the approach, in particular if you take into account the initialization time t_{init}

However, this particular approach poses a few problems. Infact if we look at how the quantity t_f/p varies for varying t_f , we discover that the minimum of such quantity will always be for the smallest t_f available, regardless of the type of hamiltonian and step function $s(t)$. The following plot does indeed show, for a few sampled γ , the shape of t_f/p . In addition, in Section ? we mentioned that when dealing with multiple runs for one search we need to take into account an initialization time t_{init} . It is thus necessary to consider a lower bound on t_f .

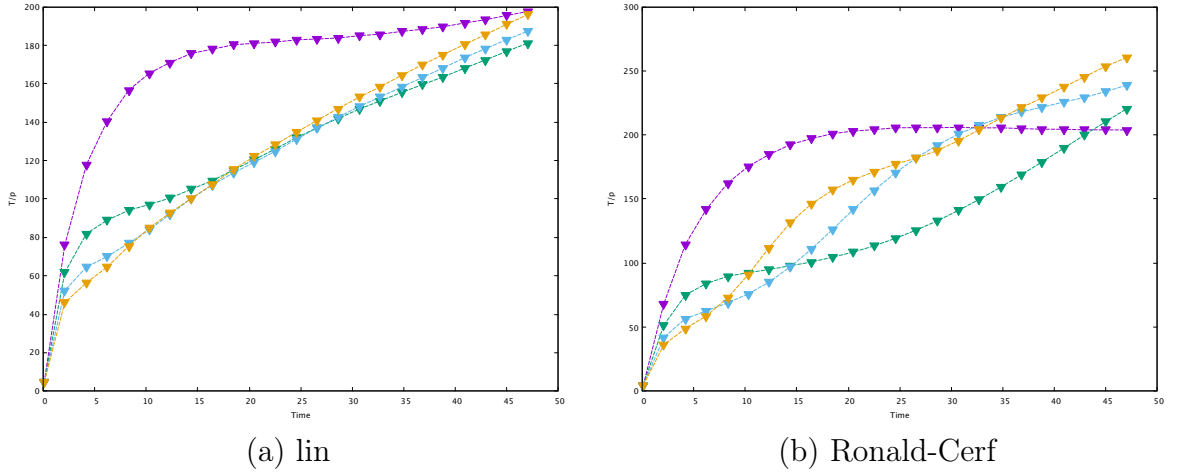


Figure 2.4: **Distribution of the quantity T/p for sampled γ showing that the $\min(T/p)$ will always be the smallest for the smallest t_f .** The figure shows the distribution of the quantity t_f/p for some sampled values of the parameter γ , using the linear and Ronald-Cerf interpolating schedules. It is clear that the quantity $\min(t_f/p)$ will always be for the smallest t_f available, regardless of the interpolating schedule, requiring therefore a constrain on the time.

$\min(t_f/p)$ and run iterations for increasing lower bound t_f

We will begin by studying how the quantity $\min(t_f/p)$ and *iters* varies with increasing lower bound t_f^* . In the following plot we show the shape of t_f/p with the time-independent approach and the time-dependent one; for the time being and for sake of semplicity, we consider only the step function Ronald-Cerf(3). As we can see from the plot the distribution can be divided into two sections marked by a particular T^* (for the time being the value of such time is not of our interest):

- for $t_f < T^*$ the time-independent approach performs slightly better than the time-dependent one.
- for $t_f > T^*$ however the time-dependent approach performs significantly better, in particular with increasing time t_f

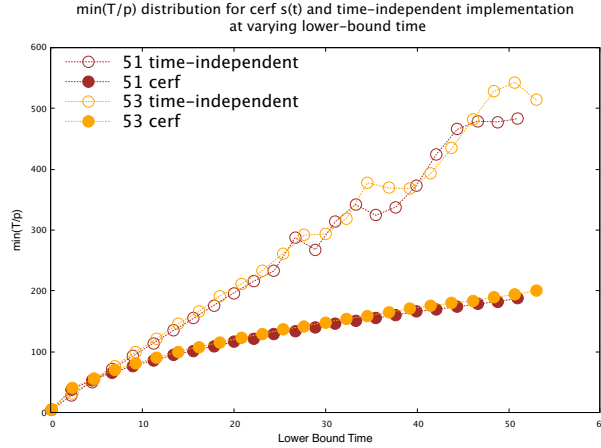


Figure 2.5: **$\min(t_f/P)$ distribution for increasing lower bound time.** The figure shows the distribution of the quantity $\min(T/p)$ for increasing values of lower bound time, using the time-independent hamiltonian (circles) and time-dependent hamiltonian (solid circles) and evaluated for a Cy(51) and Cy(53). We see that for times smaller than a characteristic time T^* the time-independent approach performs slightly better, while for large time the time-dependent one performs significantly better.

The behaviour for large T is to be expected, considering that the time-dependent approach shows localization properties and the probability increases with increasing time as we showed in Figure?, in contrast with the time-independent approach that does not show localization properties.

What this shows is that the choice of t_f has great effects on the outcome of our time-dependent approach, making it a successful or unsuccessful alternative. In terms of iterations the trend is similar to the quantity $\min(t_f/P)$, as the following plot shows.

The iterations distribution reflects the overall probability distribution of the time-dependent and time-independent hamiltonian approaches. For small lower bound time the two approaches show a similar performance: the probability is very small, thus requiring a large number of iterations to get to unitary probability. As t_f increases we see two very different trends:

- The time independent approach requires an almost constant number of iterations (the numerical values is somewhat irrelevant since this distribution reflects only the Cy(53) and Cy(55)). This reflects the non-localization properties of this particular approach, for which the probability does not increase with time
- On the other hand the time-dependent approach, showing localization properties, requires less iterations to solve the search with unitary probability.

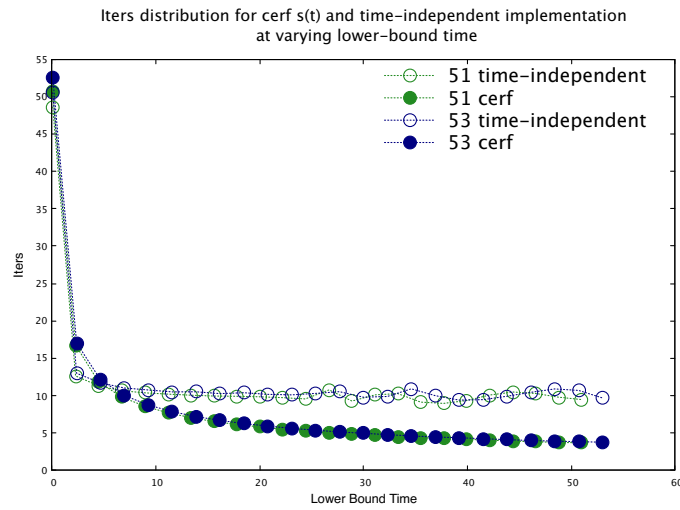


Figure 2.6: ***iters* distribution for increasing lower bound time.** The figure shows the distribution of *iters* for increasing values of lower bound time, using the time-independent hamiltonian (circles) and time-dependent hamiltonain (solid circles) and evaluated for a Cy(51) and Cy(53). This distribution reflects the probability distribution of the two approaches: for the time-independent hamiltonian the probability does not increase with time, resulting in a (almost) constant *iters*, while the time-dependent hamiltonian showing localization properties requires less iterations to get to unitary probability.

Taking into account that we're performing a multiple run search and the initialization time t_{init} previously discussed, it is clear that the time-depended approach performs better than the time-independent counter part in most of the scenario.

$\min(t_f/p)$ and run iterations with constrained lower bound time

In order to show that the lower bound time does indeed have such great impact on the performance of the time-dependent approach relative to the time-independent one we now study the distribution of the quantity $\min(t_f/P)$ with a constrain on the lower bound time.

The choice of constrain is arbitrary and somewhat biased since the larger the constrain the better the performance of the time-dependent approach, as we've just shown in fig. 2.7. Therefore, to make the choice fair, we consider the lower bound time to be $t_f^* = 2\sqrt{N}$ which is (roughly) the time scaling of the standard Grover's Search, the QW Search on the complete graph and so on. In the best case scenario we discover that the number of iterations necessary to get to unitary probability remain constant regardless of the dimension of the graph, making this approach scale as the ones just mentioned; in the most probable scenario we discover that the number of iterations increase with the graph size, thus adding a scaling factor that depends on some power of N .

The following plot shows the distribution of the quantity $\min(t_f/P)$ for circular graphs $Cy(N)$ with N up to 71. The quantity is computed using the time-dependent hamiltonian with linear step function and the time-independent one, with constrained time $t_f = 2\sqrt{N}$.

$\min(t_f/p)$ and run iterations for different shapes of $s(t)$

We now investigate the effects of the different step functions discussed in section? in the probability distribution and in particular on the quantity $\min(t_f/P)$. As we did for the general time-dependent and time-independent comparison we constrain the lower bound time to be larger than $2\sqrt{N}$. The following plot shows the distribution of the quantity $\min(t_f/P)$ for circular graphs $Cy(N)$ with N up to 71, using the time-dependent hamiltonian with linear, sqrt, cbt and Ronald-Cerf(3) interpolating schedules $s(t)$:

We can see from the plot that, as we might have expected, the Ronald-Cerf interpolating schedule performs better than the linear and sqrt schedules, in particular when we consider larger graph. For small enough N the time-independent approach performs slightly better, while for large N the time-depenedent approach is superior. Please note that the abrupt changes in the plot are due to the resolution of the grid-probability evaluation, discussed in Appendix A. *nota:*

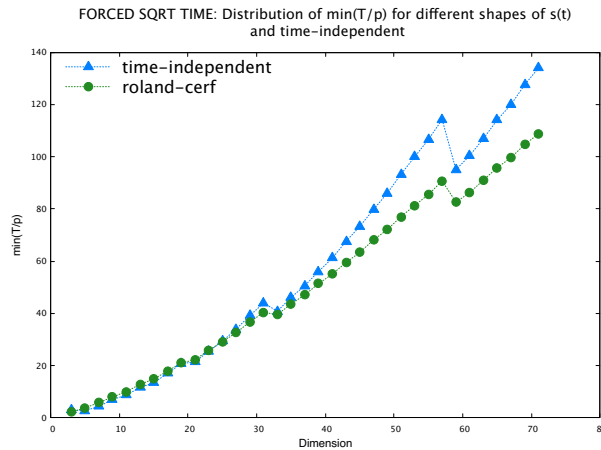


Figure 2.7: $\min(t_f/P)$ distribution for $\text{Cy}(N)$ up to $N=71$ with constrained time at $2\sqrt{N}$. The figure shows the distribution of the quantity $\min(T/p)$ for increasing values of lower bound time, using the time-independent hamiltonian (circles) and time-dependent hamiltonian (solid circles) and evaluated for a $\text{Cy}(51)$ and $\text{Cy}(53)$. We see that for times smaller than a characteristic time T^* the time-independent approach performs slightly better, while for large time the time-dependent one performs significantly better.

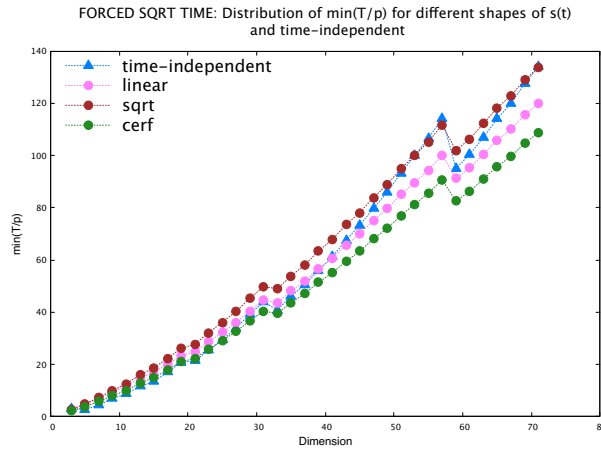


Figure 2.8: $\min(t_f/P)$ distribution for $\text{Cy}(N)$ up to $N=71$ with constrained time at $2\sqrt{N}$ and different interpolating schedules. The figure shows the distribution of the quantity $\min(T/p)$ with constrained lower bound time at $t_f = 2\sqrt{N}$, using the time-independent hamiltonian and time-dependent hamiltonian with different interpolating schedules. The abrupt changes are due to the resolution of the grid-probability evaluation (further discussions can be found in Appendix A)

Additional computations will be run to try to fix this issue.

2.4.5 Comparison: Robustness

We now address the robustness of the time-dependent and time-independent search. As we mentioned in Section? we're only interested in the comparison of the two approaches, and not an absolute measure of their robustness. Therefore we will use this measure solely as a comparison value.

We proceed by considering small variations on the parameter γ in the order of 1% and 5% (this numbers still need to be discussed). We begin by finding the quantity $\min(t_f/P)$ with time constrains ($t_f = 2\sqrt{N}$). For the corresponding (t_f, γ) combination we evaluate the robustness R as defined in Section?. For the time-dependent search with only consider the linear step function an the Ronal-Cerf(3). As we showed in the previous section the Ronald-Cerf Hamiltonian performs better than the linear conterpart, while from a qualitative point of view the linear hamiltonian has a smoother probability distribution (see fig. 2.3(a)-(d)). The following plots show the semi-quantitative robustness for the γ variations in the order of 1% - 5% for the time-independent search and the time-dependent one with linear and Ronald-Cerf step functions $s(t)$. **Computations are still needed**

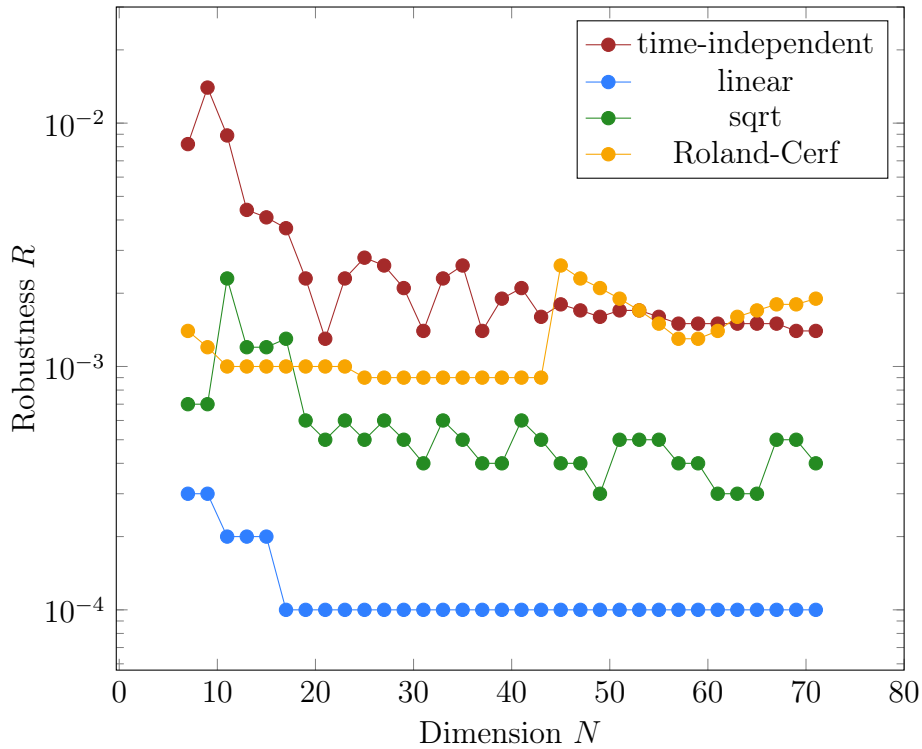


Figure 2.9: Test plot

2.5. Results for the Complete Graph

2.5.1 Search results from Wong(2016)

2.5.2 Localization results

Conclusions

Appendices

Appendix A: Probability Grid Evaluation

Appendix B: Computational Routines

In this section an overview of the computational methods is presented, focusing the attention on the **optimization algorithm** and the **differential equation solver**. Additionally the normalization error is discussed. Lastly computational reasoning for the **probability grid evaluation** are presented.

Most all numerical simulations were performed using **Python**. Numerical methods such as optimization and ODE Solver come directly from python's native **Scipy**. In addition, a CPU-multiprocessing library, **Ray**, has been used to speed up the grid probability evaluation quite noticeably. Heatmap plots were created using python matplotlib, while additional plots were created with gnuplot.

2.5.3 Optimization Algorithm

In Section III a series of benchmark were performed to compare the time-dependent and time independent hamiltonian approach to the search problem. In order to determine which optimization algorithm fitted the best for the task, a number of possible algorithm were tested, such as *shgo*, *dualannealing*, *minimize*, *LHSBH* and *Basin-Hopping*.

Due to the oscillating nature of the probability (**a figure is needed**) the scipy native **Basinhopping algorithm** was used. As the name suggests the algorithm performs a series of randomized hops, i.e. jumps, of the coordinates in order

to find the true maximum This fits particularly well with the series of maxima and minima of the probability function (for fixed γ) in the time-independent hamiltonian.

Additional information on the parameter used are needed (e.g. step size, number of iterations)

2.5.4 Schroedinger Solver and Normalization Error

In Section II we presented an evolution which is governed by a time-dependent hamiltonian, used to find the evolved state $|\psi(t)\rangle$. This is accomplished by solving the usual Schroedinger equation using Scipy's `integrate.solve_ivp`, that provides a wide varieties of integrations methods.

As it's routine we used Runge-Kutta RK45, which as stated in the documentation it's a explicit Runge Kutta method of order 4(5). The error is controlled assuming fourth order accuracy, but steps are taken using the fifth-order accurate formula. In addition, the integrator is adaptive, meaning that the time step is chosen for optimal error control. Regarding the error, the algorithm provides two distinct parameters to set a targeted limit, namely the **relative (rtol)** and **absolute tolerances (atol)**. The first provides a relative accuracy, i.e. the number of digits, while the latter is used to keep the local error estimate below the threshold $atol + rtol*abs(y)$. Determining the correct combinations of the two parameters is key for achieving the desired error. A few of those are presented in the following table, where a worst case scenario (N=101, T=1000) is used and the error is evaluated on the expected normalized state. The combination of rtol and atol bolded is the one we used in the solver, which gives us a small enough error on the normalization without greater computational expense.

Bibliography

- [1] A. M. Childs, E. Farhi, and S. Gutmann. An example of the difference between quantum and classical random walks. (2):1–4, 2001.
- [2] A. M. Childs and J. Goldstone. Spatial search by quantum walk. *Physical Review A - Atomic, Molecular, and Optical Physics*, 70(2), 2004.
- [3] E. Farhi, J. Goldstone, S. Gutmann, and M. Sipser. Quantum Computation by Adiabatic Evolution. 2000.
- [4] L. K. Grover. Quantum mechanics helps in searching for a needle in a haystack. *Physical Review Letters*, 79(2):325–328, 1997.
- [5] J. G. Morley, N. Chancellor, S. Bose, and V. Kendon. Quantum search with hybrid adiabatic?quantum walk algorithms and realistic noise. pages 1–24, 2018.
- [6] O. Mülken and A. Blumen. Continuous-time quantum walks: Models for coherent transport on complex networks. *Physics Reports*, 502(2-3):37–87, 2011.
- [7] M. A. Nielsen and I. L. Chuang. *Quantum Computation and Quantum Information*. Cambridge University Press, 2000.
- [8] J. Roland and N. J. Cerf. Quantum search by local adiabatic evolution. *Physical Review A - Atomic, Molecular, and Optical Physics*, 65(4):6, 2002.
- [9] S. Z. SH. Hung, S. Hietala. Quantitative Robustness Analysis of Quantum Programs (Extended Version). *Proceedings of the ACM on Programming Languages*, 3(January), 2019.

- [10] T. G. Wong and D. A. Meyer. Irreconcilable difference between quantum walks and adiabatic quantum computing. *Physical Review A*, 93(6):1–8, 2016.